

## VIBRATION SMALL ARM BARREL

Peter PERUN<sup>1</sup>\*

<sup>1</sup> Peter PERUN, Department of Engineering, Armed Forces Academy of general M.R.ŠTEFÁNIK, Demänová 393, 031 01 Liptovský Mikuláš

\*Corresponding author E-mail address: peter.perun@aos.sk

### Abstract

Muzzle vibration of small arm during shoot is caused by projectile motion in navigate part of small arm barrel. Amplitude of muzzle vibration depends on barrel material, barrel production technology, constructional solution of arm automatics, type and quality ammunition. Size variations muzzle at the moment of the shot directly affects the accuracy of fire.

By exchange of inside and outside barrel loading come to exchange of muzzle vibration magnitude during shoot. To small arm muzzle vibration detection was carried out the experiment by shooting. The weapon was loaded with shooting during which the size deflection of the small arm barrel was measured by the vibrodiagnostic device.

To small arm muzzle vibration detection was created model of small arm barrel with accessories in program LS-Dyna. Model of small arm barrel come out of proportions and material of small arm Sa vz.58. Barrel accessory creates front sight carrier and gas chamber. Both components represent addition mass to barrel without accessories, that are change muzzle oscillation character. Model of small arm barrel is loaded by inside forces affect during shoot. There are, press of burning powder gases and reaction of projectile moving in barrel.

Goal is comparison size deflection of muzzle small arm barrel model, versus size deflection of muzzle small arm barrel weapon Sa vz.58 from experiment.

**Keywords:** Barrel vibration, muzzle, small arms barrel model, simulation.

### 1 Introduction

Muzzle vibration of small arm during shoot is caused by projectile motion in navigate part of small arm barrel. Amplitude of muzzle vibration depends on barrel material, barrel production technology, constructional solution of arm automatics, type and quality ammunition. Size variations muzzle at the moment of the shot directly affects the accuracy of fire.

By exchange of inside and outside barrel loading come to exchange of muzzle vibration magnitude during shoot. To small arm muzzle vibration detection was carried out the experiment by shooting. The weapon was loaded with shooting during which the size deflection of the small arm barrel was measured by the vibrodiagnostic device.

### 2 Creating a model

To determine the size of the deflection of the small bore barrel, a small bore barrel model was constructed mainly in the LS-Dyna program. The small bore barrel model mainly comes out of the dimensions and material of the barrel of the 7.62 mm automatic assault rifle Sa vz.58. The model is supplemented with barrel accessories and compensator (Fig.1). The model is composed out of a sight carrier ( $m_{nm}= 72.10^{-3}$ kg), a gas chamber ( $m_{pk}= 82.10^{-3}$ kg) and a compensator ( $m_{kz}= 118.10^{-3}$ kg). The components represent the added weight to the bare barrel, which changes the character of the oscillation of the muzzle. The function of accessory components does not interfere with or affect the oscillation of the small bore barrel. For example, by influencing of the oscillation by the motion of the gas piston, or by discharge of dust emissions through the holes on the compensator. [2],[7],[9],[10]

The small bore barrel model is mainly influenced by the internal forces acting during the shot. They represent the pressure of the burning dust gases and the reaction from the missile movement in the barrel.

By using attachments to the muzzle of the small bore barrel such as a noise silencer (suppressor), rise compensators and flame silencers there is a further change in the oscillation the small bore barrel. The size of the deflection of level of the muzzle will be affected by the added weight at the mouth.

The small bore barrel model is created on the dimensions and materials characteristics of 7.62 mm muzzle of assault rifle Sa vz.58 currently implemented in the Armed Forces of Slovak Republic (Fig. 6). The LS-Dyna software was used to build the model. The model has four versions.

To determine the value of the plane deflection of the muzzle of the small bore barrel model, especially at the moment when the shot leaves the guiding section of the barrel there are four defined NODs: A, B, C, D. They are located in the plane of the muzzle at the end of the end of the guiding elements of the boring of the small bore barrel model.



*Fig. 1 Gas chamber, front sight carrier, compensator*

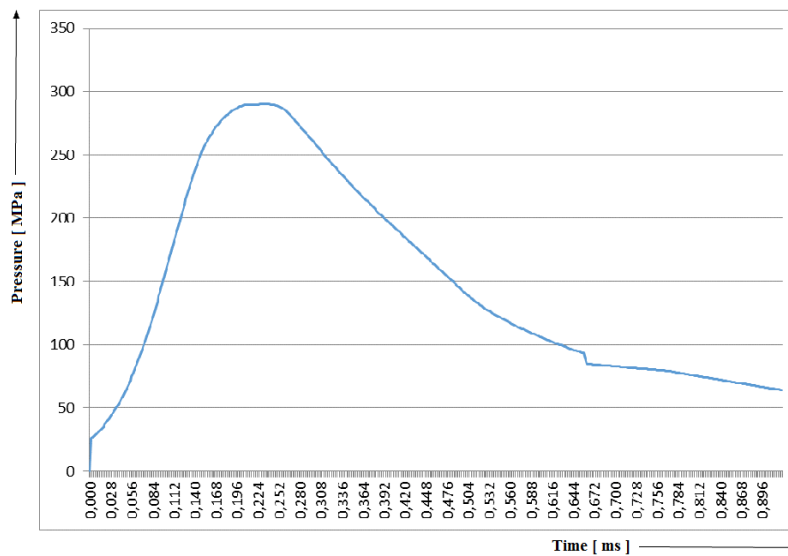


*Fig. 2 Progress of the pressure in the barrel*

All the versions of the small bore barrel model are firmly fixed into the casing of end of the gun in the length of 62mm. They are loaded with a pressure load according to the pressure curve in the barrel (Fig.2). The curve of the pressure pattern corresponds to the 7.62 mm x 39 vz.43 bullet gun shot, with a shot of 8 g FMJ, 1,58 g content of tube nitrocellulose smokeless powder from S&B company, at temperature  $t_v=20^{\circ}\text{C}$ , pressure  $p_n=1011,5\text{ hPa}$ . [3],[4].

The motion time of 7.62 mm bullet in the guide portion of the bore of the model until the moment when it leaves the muzzle of the small bore barrel model is  $t_{sh} = 0,91\text{ ms}$ . The material of the small bore barrel model has the following parameters: density  $\rho=7850\text{ kg}\cdot\text{m}^{-3}$ , Young's modulus  $E=2,1\cdot 10^3\text{ MPa}$ , Poisson constant  $\mu=0,3$ .

### 3 Small arms barrel model

In this section it is necessary to present in details assumptions and the course of authors' research to such an extent that a reader could repeat those steps to confirm achieved results. In short papers this information should be given as briefly as possible All models of small bore barrel are created in the LS - Dyna program based on the original 7.62 mm automatic attack rifle Sa vz.58. Individual variants differ from each other by the absence of accessory components or by their presence. The small bore barrel models are loaded by the pressure load of the burning dust gases and the load from the movement of the missile in the guiding part. [2],[3],[4]

The first small bore barrel model is without accessories (Fig.3). From the original barrel of small bore weapon, only the external and internal dimensions remained. This model is without a gas piston, gas chamber, and a sight carrier with a bayonet carrier.

The second small bore barrel model is without accessories (Fig.4). From the original barrel of small bore weapon, only the external and internal dimensions remained. This model is without a gas piston, gas chamber, and a sight carrier with a bayonet carrier. At the muzzle, the model is has extra weight in form of a compensator (Fig.1).

The third small bore barrel model with accessories (Fig.5) This model is identical with the original small bore barrel, external and internal dimensions remained. The model of the small bore barrel contains gas chamber, sight carrier and bayonet carrier (Fig.1).

The last small bore barrel model is with accessories. (Fig. 6) The model is identical with the original small bore barrel weapon, the external and internal dimensions remained. The small bore barrel model contains gas chamber, sight carrier, bayonet carrier, including a screwed-in compensator (Fig. 1).

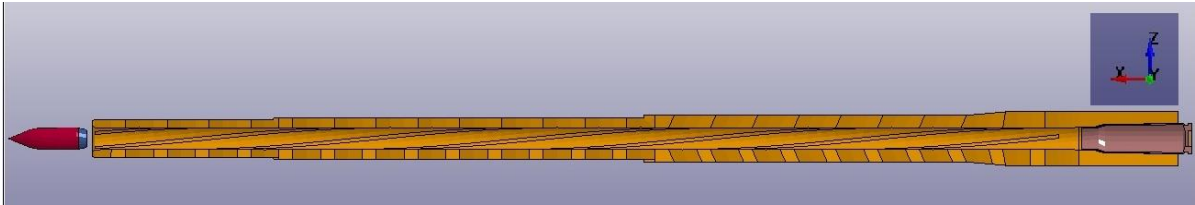


*Fig. 3 Model small arms barrel without accessories*

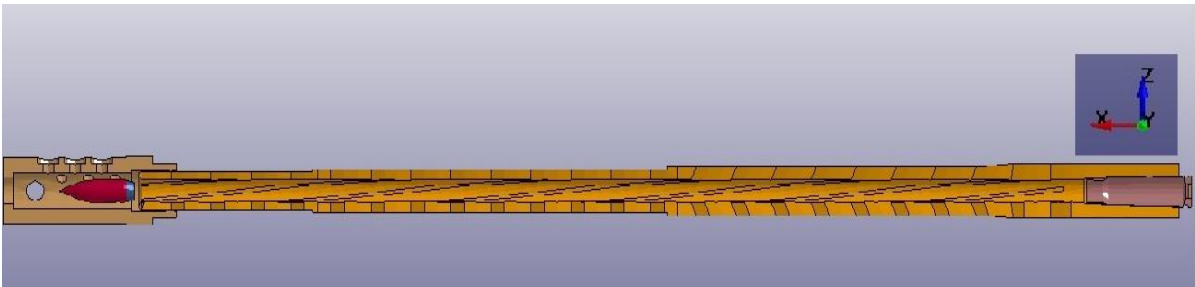


*Fig. 4 Model small bore barrel without accessories with compensator*

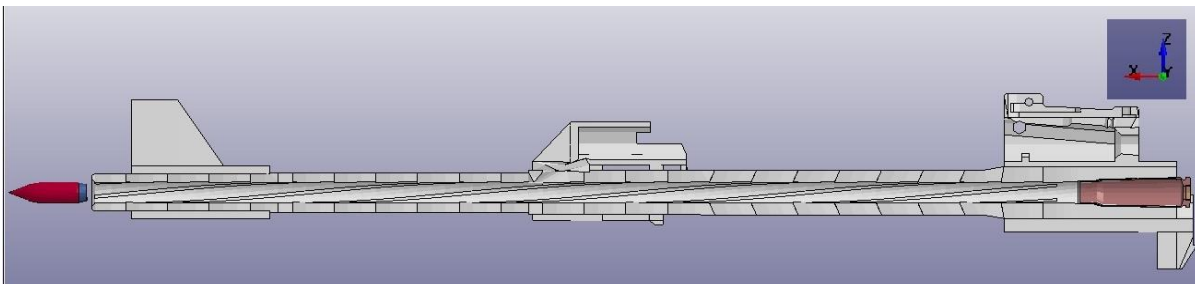


*Fig. 5 Model small bore barrel with accessories*

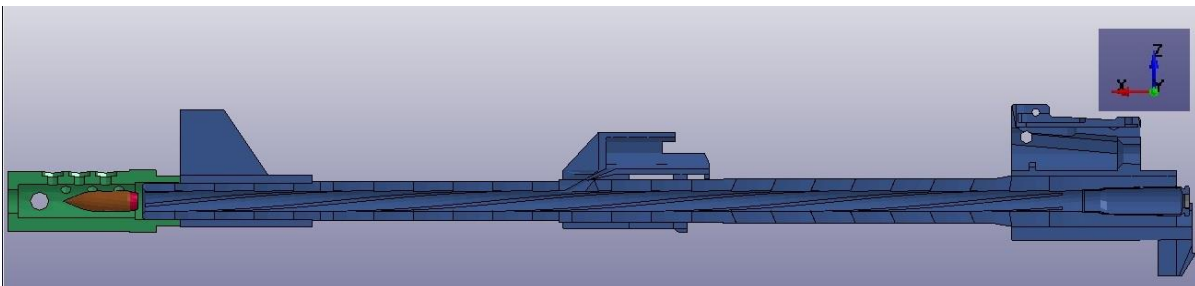


*Fig. 6 Model small bore barrel with accessories with compensator*

#### 4 Simulations

On all small bore barrel models, a simulation with a pressure load and simulation with missile movement in the guiding part of the barrel was performed. The simulation is tasked to approximate to the real shooting conditions from the 7,62 mm assault rifle Sa vz.58 as much as possible.

*Table 1 Deflection values of the NODs at the muzzle barrel.*

Deflection axis	Deflection values of the NODs at the muzzle barrel [ mm]			
	A <sub>1</sub>	B <sub>1</sub>	C <sub>1</sub>	D <sub>1</sub>
axis – x	0,000159	-0,00369	-0,00244	0,00253
axis – y	0,02	0,0096	0,00187	0,012
axis – z	-0,0114	-0,0166	-0,006	-0,000185

**Table 2** Deflection values of the NODs at the muzzle barrel

Deflection axis	Deflection values of the NODs at the muzzle barrel [ mm]			
	A <sub>2</sub>	B <sub>2</sub>	C <sub>2</sub>	D <sub>2</sub>
axis – x	0,000153	0,00259	0,00333	0,00134
axis – y	0,000878	-0,00522	-0,0102	-0,00410
axis – z	0,00648	0,00258	0,00945	0,0128

**Table 3** Deflection values of the NODs at the muzzle barrel

Deflection axis	Deflection values of the NODs at the muzzle barrel [ mm]			
	A <sub>3</sub>	B <sub>3</sub>	C <sub>3</sub>	D <sub>3</sub>
axis – x	0,0000305	0,00247	-0,000214	-0,00275
axis – y	-0,0081	-0,0143	-0,0197	-0,0151
axis – z	-0,00427	-0,00933	-0,00391	0,00202

**Table 4** Deflection values of the NODs at the muzzle barrel

Deflection axis	Deflection values of the NODs at the muzzle barrel [ mm]			
	A <sub>4</sub>	B <sub>4</sub>	C <sub>4</sub>	D <sub>4</sub>
axis – x	-0,00061	0,000061	-0,000549	-0,00125
axis – y	-0,00555	-0,00733	-0,00928	-0,00746
axis – z	-0,00177	-0,00375	-0,00167	0,000409

The obtained values of deflections in the muzzles of the models in time  $t_{sh} = 0,91$  ms for axes  $x, y, z$  were inserted into the tables Table 1, Table 2, Table 3, Table 4. [1],[6]

### 5 Experiment

Measuring device (Fig.7) consisting of several elements was built out of ideal laboratory conditions by the open range.

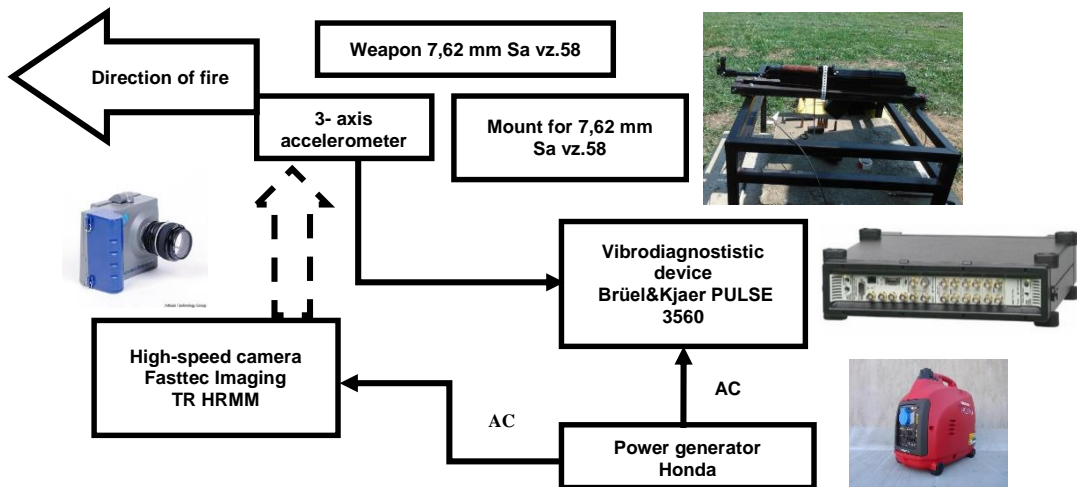


**Fig.7** Measuring chain



**Fig.8** Assault rifle SA vz.58P

All elements of the measuring devices were placed and ready for action in the body of an open shooting range firing line along the paved surface.

For supply of measuring, recording and evaluating elements of the measurement chain electricity was used for four-stroke generator.

The measuring chain comprises a gun 7.62 mm assault rifle Sa vz.58P (Fig.8) with accelerometer clamped on the barrel weapons. Tripod to consolidate weapons. Vibrodiagnostic equipment Brüel & Kjær PULSE 3560 with base plate for connecting a notebook with accelerometer control and evaluation software. High-speed cameras Fastec Imaging TR HRMM.

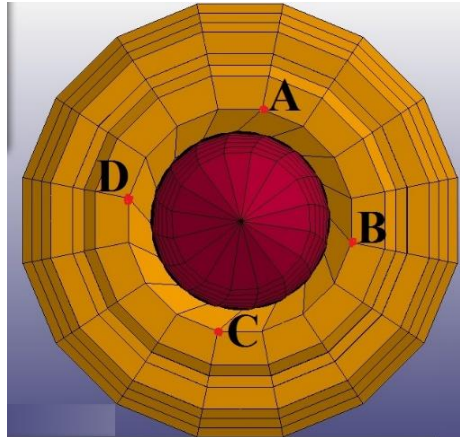


Fig. 9 Location NOD on the model barrel muzzle

Measures were carried on the gun 7.62mm assault rifle Sa vz. 58P for external conditions:  $t_v = 21^\circ\text{C}$ ,  $p_N = 1011.5 \text{ hPa}$ , humidity 65%. Was used to fire ammunition 7.62 mm x 39 vz.43, 8 grams FMJ bullet, from S&B. The weapon has been disabled firmly on the stand for the end of the breech. Tripod was loaded with concrete blocks with a total weight of 100 kg.

The aim of the experiment was obtained by measuring the size of deflection of the barrel set of data after processing could be further exploited. Measurement objectives have been achieved and the measurement results as graphs during deflection of the muzzle for the duration of the shot i.e. from the moment of initiation charge up to the moment when the shot leaves the guide of the head.

Table 5 Deflection values from accelerometer at the muzzle barrel

Deflection axis	Deflection values of muzzle barrel [ mm]	
	C <sub>5</sub>	C <sub>6</sub>
axis – x	0,89	0,54
axis – y	0,46	0,21
axis – z	-0,12	-0,094

From the measured data, the velocity variations of the orbital plane were selected mainly in the x, y, z levels at time  $t_{sh} = 0.91 \text{ ms}$ . The data were placed in Table 5. The size of the orbital plane deflections in planes x, y, z apply to the barrel without the compensator are designated for the data group C<sub>5</sub> and the barrel with the compensator for the data set C<sub>6</sub>.

## 6 Discussion of results

For the purpose of comparing the velocity variations of the orbital plane of the individual simulations, the data from Table 1, Table 2, Table 3, Table 4 of the C-NODs group were selected. The date were inserted into the common Table 6 together with the data measured during the experiment found in Table 5.

Table 6 Deflection values of the NODs at the muzzle barrel

Deflection axis	Deflection values of the NODs band of C at the muzzle barrel [ mm]					
	C <sub>1</sub>	C <sub>2</sub>	C <sub>3</sub>	C <sub>4</sub>	C <sub>5</sub>	C <sub>6</sub>
axis – x	-0,00244	0,00333	-0,000214	-0,000549	0,89	0,54
axis – y	0,00187	-0,0102	-0,0197	-0,00928	0,46	0,21
axis – z	-0,006	0,00945	-0,00391	-0,00167	-0,12	-0,094

Data from the simulation were selected from the C-NODs group because the accelerometer was located at the lower part of the mouth during the experiment. This corresponds to the positioning of the C-NODs group on the

model of the barrel muzzle. (Fig.9). The accelerometer could not be placed simultaneously at the other positions corresponding to the NOD groups of A, B, D, from the simulation because it would affect the measurement of the deviation of the plane of the muzzle by the added weight.

The graphs (Fig.10, Fig.11) were composed from the scale variations of the C-NODs group on the muzzle of the model and the velocities of the plane of muzzle of real barrel without the compensator and with the stroke compensator listed in Table 6.

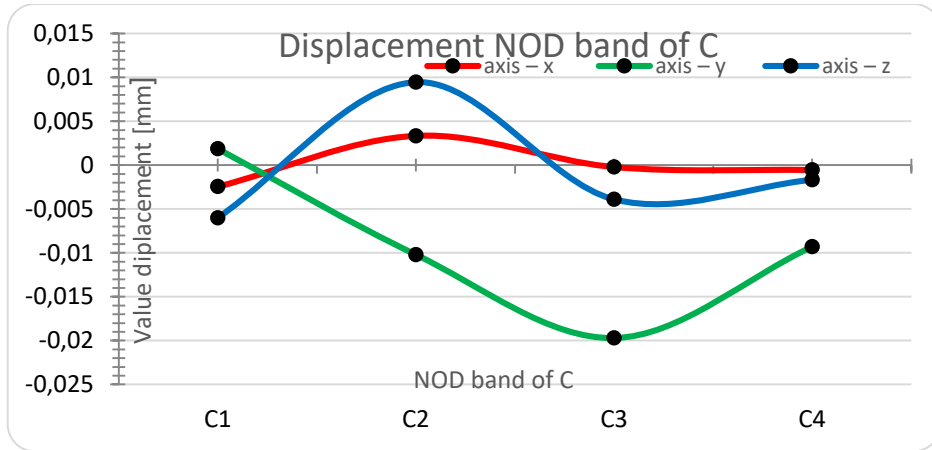


Fig. 10 Displacement of C NOD from simulation

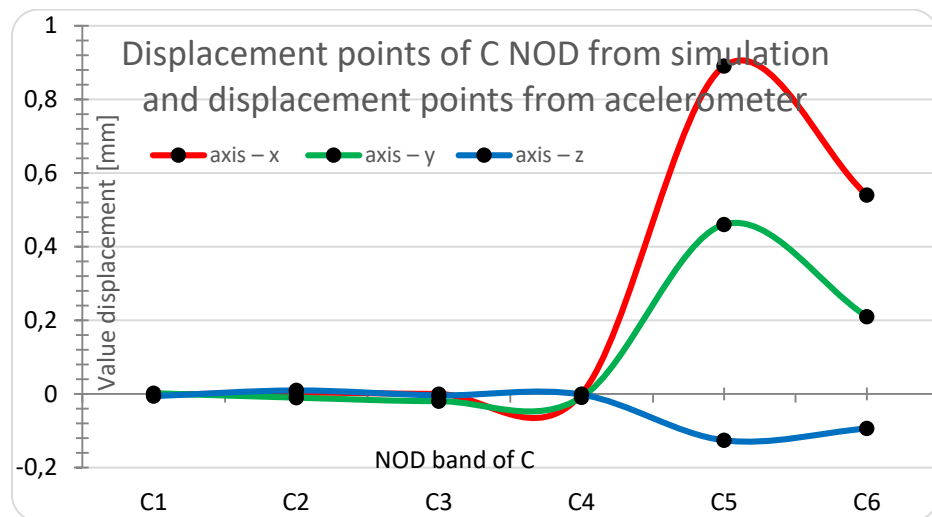


Fig. 11 Displacement of C NOD from simulation and displacement point from accelerometer

## 7 Conclusion

The same is true for the real weapon SA model 58. For the time  $t_{sh} = 0,91$  ms, there is an oscillation of the small bore barrel model as well as of the real weapon in the  $x$ ,  $y$ ,  $z$  axes. The oscillation is of non-linear nature. The largest deflection values have been recorded from  $y$ -axis and  $z$ -axis (horizontal and vertical plane). The smallest deflection values are recorded in the  $x$ -axis (boring of the barrel) (Fig.10).

Another situation occurred for the measured deflections of the real weapon. The largest deflections were measured at time  $t_{sh} = 0,91$  ms in the  $x$ -axis, probably due to the small stiffness of the gun-carriage fastener. Smaller deflections were in the  $y$ ,  $z$  axes (Fig.11)

At the time when the missile leaves the mouth, the situation with NOD-deflection sizes in A, B, C, D NODs in the plane of the muzzle is similar. The largest deflection values have been recorded from  $y$ -axis and  $z$ -axis; the smallest deviation values have been recorded in the  $x$ -axis.

The Table 1 shows the fact that the small bore barrel model with no accessories (Fig.3) at time  $t_{sh} = 0,91$  ms has the largest variations in the  $y$ -axis of the NOD  $A_1$ .

Adding the compensator (Fig.1) will reduce the NOD deflection in  $A_2$ ,  $B_2$ , but at the same time increase the displacement NOD in  $C_2$ ,  $D_2$  (Fig.4) The compensator partially full fills the function of the damping element. The same situation occurred with the real weapon and compensator, where compared to the no - compensator variant,



there was a reduction of the deflections in the plane of the muzzle of the weapon (Fig.11). This applies to C<sub>6</sub> group deflections.

Model variation of the barrel with accessories (Fig.5) shows increased variations in all A<sub>3</sub>, B<sub>3</sub>, C<sub>3</sub>, D<sub>3</sub> NODs Table 3. compared to previous variants. This also applies for the deflection group of the C5 experiment with the barrel without the compensator (Fig.11).

From the point of view of the extent of deflection, the most favourable is the variant of the barrel model with the accessories and the compensator (Fig.6). The deviations of all A<sub>4</sub>, B<sub>4</sub>, C<sub>4</sub>, D<sub>4</sub> NODs Table 4 are the smallest almost in all x, y, z axes, The reason is probably the size of added weight in the form of accessories and compensator, as well as the distribution of added weight itself.

It follows from the above mentioned facts that general solidity of the barrel and the size of added weight at the barrel muzzle plays the key role in the extend of deflection of the plane of the muzzle at time t<sub>sh</sub>.

The ideal situation would be to choose the right amount of the added weight and its distribution through the modular solution of the muzzle device. The muzzle device could be in a form of a compensator, or a suppressor with a possibility to add the loading and to change its position. The purpose would be zero or only a minimal deflection of the muzzle, which would favorably affect the accuracy of shooting.

#### References:

- [1] LISÝ,P. – ŠTIAVNICKÝ,M.: Modal Analysis od Barrel for Assault Rifles. In: Problems od Mechatronic, 2(8)2012, p.7, , ISSN 2081-5891.
- [2] LISÝ,P. – ŠTIAVNICKÝ,M.: Weapons Barrel and its additional Accessories. In: Problems od Mechatronic, 5,1 (15) 2014,č.2 p.9, ISSN 2081-5891.
- [3] PERUN,P. – MOZOLA,M.: Comparision of vibrations models of small arms barrels. In: Deterioration Dependability Diagnostics, UO Brno, 2016, p.139, ISBN 978-80-7231-1.
- [4] PERUN,P.: Comparision small arms barrel vybration with simulation. In:Zeszyty Naukove Institutu Pojazdów, Warszawa,3(107)/2016, p.63, ISSN 1642-347X.
- [5] SCHWINKENDORF, K. N. and S. P. ROBLYER, 1998. Three River Technologies – Simulation of the Vibrational Response of a Barrel Rifle During Firing. In: *Advance Simulation Technologies Conference (ASTC '98)*, p. 66.
- [6] REDDY, N.J.: Finite Element Method. New York, 2006. 766 s.
- [7] VARMIT,A.:FEA (Finite Element Analysis) Rifle Barrel Dynamic Pressure Analysis. <http://varmintal.com/apres.html>
- [8] TREBUŇA, F. – JURICA, V. – ŠIMČAK, F.: Pružnosť a pevnosť II. Prešov, 2002. 318 s
- [9] VÍTEK, R.: Influence of the Small Arm Barrel Bore Length on the Angle of Jump Dispersion. In: Proceedings of the 7th WSEAS International Conference on Systeme science andsimulation in engineering ICOSSE'08. Wisconsin: WSEAS, 2008, p. 114-118.
- [10] LISÝ,P. – ŠTIAVNICKÝ,M.: The barrrel and its additional accessories. In: 9th International Armament Conference on Scientific aspects od armament &safety technoogi, 28-28. september 2012 Pultusk – Varšava, Wojskova Akademia Techniczna 2012, s.485-497.
- [11] RINKER, A. R., 2009. *Understading Firearm Ballistics*. Mulbery House Publishing, p. 430. ISBN: 978-0964559844.
- [12] ŠTIAVNICKÝ, M. and P. LISÝ, 2013. Influence of Barrel Vibration on the Barrel Muzzle Position at the Moment when Bullet Exits Barrel. In: *Advances in Military Technology*. Vol. 8, No. 1.
- [13] HUA, H., Z. LIAO and J. SONG, 2015. Vibration reduction and firing accuracy improvement bynatural frequency optimization of a machine gun system. In: *Journal of Mechanical Science and Technology*. 29 (9), p. 3635-3643.
- [14] GIMM, H. I., K. U. CHA and CH. K. CHO, 2012. Characterizations of gun barrel vibrations of during firing based on shock response analysis and short-time Fourier transform, In: *Journal of Mechanical Science and Technology*. 26 (5), p. 1463-1470.
- [15] ESEN, I. and M. A. KOÇ, 2015.Optimization of a passive vibration absorber for a barrel using the genetic algorithm. In: *Scence Direct, Expert Systems with Applications*. 42 (2015), p. 894–905.
- [16] DENG, S., H. K. SUN and Ch. J. CHIU, 2012. Rifles in – bore finite element transient analysis. In: *Proceedings of the International Conference on Mechanical, Production and Materials Engineering (ICMPME 2012)*. Bangkok, 16 - 17 June 2012, p. 58-62.
- [17] JEDLICKA, L., S. BEER and M. VIDENKA, 2008. Modelling of pressure gradient in the space behind the projectile. In: *Proceedings of the 7th WSEAS International Conference on System Science and Simulation in Engineering - ICOSSE '08*. Wisconsin, p. 100-104.
- [18] KAY, M. J., P. D. DEWITT, L. T. BERGMAN and S. A. LAVINE, 2007. *Fundamentals of Heat and Mass Transfer*. John Wiley&Sons, p. 997.